

Thermo-Electric Figure of Merits ZT of the Thick Rectangular PBTE Nano-Wire by Considering Acoustic Phonon Scattering Beyond Size Quantum Limits

M P Singh¹

¹Professor, Physics Department, Rajkiya Mahila Mahavidyalaya Shahganj, Jaunpur, India
Corresponding Author: singhm74@gmail.com

Abstract: In the paper, we have study thermo-electric figure of merits ZT of thick rectangular PbTe nanowire by the formulation based on the Boltzmann relaxation time approach for acoustic phonon scattering. In PbTe nanowire beyond size quantum limit thermoelectric figure of merits optimum for the diameter of the wire in the range 75nm-125nm and operating temperature range of the device 300K-800K. The high value of ZT expected at lower concentration of the carrier and optimum cross-sectional size of the nanowire. The PbTe nanowire are useful for geothermal energy generation.

Keywords: PbTe, nano-structures, electronic transport, nano-wires.

1. Introduction

The efficiency of the thermoelectric engine is the product of the Carnot efficiency $\eta_c = \frac{T_H - T_C}{T_H}$ and $\gamma = \frac{\sqrt{1+Z\bar{T}}-1}{\sqrt{1-Z\bar{T}}+\frac{T_C}{T_H}}$ $\bar{T} = \frac{T_H + T_C}{2}$ which is depends on the figure-of-merits of the materials. The concept of a dimensionless figure-of-merit for a material is employed and given by $ZT = \frac{\alpha^2 \sigma}{k_e + k_L} T$ the term $\alpha^2 \sigma$ refers electrical power factor, α Seebeck coefficient (Thermo-power), σ electrical conductivity, k_L lattice contribution to thermal conductivity and k_e electronic thermal conductivity[1-14]. The Lead telluride is in bulk a good thermoelectric materials in the category polar semiconductor with ionic-covalent bonds. Its structure is m3m symmetry NaCl type face centred cubic crystallize structure. The high degree of freedom of PbTe quantum wire on constant energy surfaces are due to multiplicity and high anisotropy. For high efficiency thermoelectric devices must have high Seebeck coefficient and electrical conductivity, and low thermal conductivity. For optimisation of figure of merit is choice of such a materials which have character as phonon glass and electron crystal. The confinement of carrier in order of deBroglie wavelength of the carrier create new characteristics of the material. When

confinement in two directions in order of deBroglie wave length and carrier are free to move in one direction the conduction band are quantised into sub-bands. Due to quantisation in sub-bands multiple modes of transportations are produces. These sub-bands change the transport behaviour. As electron passes along the nanowire with all boundary with its mean free path increases resistivity. The transverse dimensions comparable to mean free path enhance the electron phonon scattering, electron-electron scattering at low temperature due to collision by surfaces [15-21]. In this paper we discuss multiple mode contribution in ZT of PbTe thick nanowire.

2. Theory

In polar semiconductor both acoustic scattering and optical phonon scattering play significant role at high temperature.

The relaxation time for acoustic phonon scattering one-dimensional systems is may be expressed as [21]

$$\tau_{nl}(k) = \frac{4}{9} \frac{\hbar^2 c_{11} ab}{2\varepsilon_1^2 (k_B T) (2m^*)^{\frac{1}{2}}} \varepsilon^{\frac{1}{2}}$$

Here c_{11} is the longitudinal elastic constant and ε_1 is the deformation potential, $\varepsilon = E - E_c$,

$$\tau = \tau_0 \varepsilon^p$$

For acoustic phonon scattering $p = \frac{1}{2}$; $\tau_0 = \frac{4\hbar^2 c_{11} ab}{18\varepsilon_1^2 k_B T (2m_z^*)^{\frac{1}{2}}}$

The PbTe nanowire consider in the form of a rectangular wire which characterised by transverse dimensions 'a' and 'b' and a wire of length L along the z-axis. The Transport coefficients for such a system are given by such as electrical conductivity, Seebeck coefficient, and the electronic contribution to thermal conductivity given as: [10-12]

$$(01) \sigma = \frac{2\tau_0 e^2}{\pi \hbar ab (2m_z^*)^{1/2}} B_6$$

$$(02) \alpha = \frac{k_B}{e} \left[\frac{E_F}{k_B T} - \frac{B_4 + B_5}{k_B T B_6} \right]$$

$$(03) k_e = \left(\frac{k_B}{e} \right)^2 \left[\frac{B_1 + 2B_2 + B_3}{(k_B T)^2 B_6} - \left(\frac{B_4 + B_5}{k_B T B_6} \right)^2 \right] \sigma T$$

where $B_1, B_2, B_3, B_4, B_5,$ and B_6 are given by

$$(04) B_1 = \sum_n \sum_l \left(p + \frac{5}{2} \right) (k_B T)^{\left(p + \frac{5}{2} \right)} F_{\left(p + \frac{3}{2} \right)}(\eta_{n,l})$$

$$(05) B_2 = \sum_n \sum_l (E'_n + E'_l) \left(p + \frac{3}{2} \right) (k_B T)^{\left(p + \frac{5}{2} \right)} F_{\left(p + \frac{1}{2} \right)}(\eta_{n,l})$$

$$(06) B_3 = \sum_n \sum_l (E'_n + E'_l)^2 \left(p + \frac{1}{2} \right) (k_B T)^{\left(p + \frac{5}{2} \right)} F_{\left(p - \frac{1}{2} \right)}(\eta_{n,l})$$

$$(07) B_4 = \sum_n \sum_l \left(p + \frac{3}{2} \right) (k_B T)^{\left(p + \frac{3}{2} \right)} F_{\left(p + \frac{1}{2} \right)}(\eta_{n,l})$$

$$(08) B_5 = \sum_n \sum_l (E'_n + E'_l) \left(p + \frac{1}{2} \right) (k_B T)^{\left(p + \frac{3}{2} \right)} F_{\left(p - \frac{1}{2} \right)}(\eta_{n,l})$$

$$(09) B_6 = \sum_n \sum_l \left(p + \frac{1}{2} \right) (k_B T)^{\left(p + \frac{1}{2} \right)} F_{\left(p - \frac{1}{2} \right)}(\eta_{n,l})$$

where $F_{(p)}(\eta_{n,l})$ is Fermi-integral defined as

$$(10) F_{(p)}(\eta_{n,l}) = \int_0^\infty \frac{x^p}{\exp(x - \eta_{n,l}) + 1} dx$$

$$E'_n = \frac{E_n}{k_B T} \quad E'_l = \frac{E_l}{k_B T}, \text{ reduced carrier energy } x = \frac{\varepsilon}{k_B T}$$

with respect to conduction band edge, $\eta_{n,l} = \xi - E'_n - E'_l$; reduced Fermi energy $\xi = \frac{E_F}{k_B T}$. Here summation taken over several sub-bands.

The total thermal conductivity is given by

$$k = k_e + k_L$$

Thermal conductivity studies on Silicon nanowire cross-sectional diameters reveal that phonon confinement results in a significant reduction in phonon contribution to thermal conductivity, $k_{nw} = 0.1 k_{bulk}$ [14-19]. Assuming a similar situation for Lead telluride we estimate a highly approximate value of phonon thermal conductivity $\approx 0.17 W m^{-1} K^{-1}$. The dimensionless figure-of-merit is given by

$$ZT = \frac{\alpha^2 \sigma}{k_e + k_L} T$$

3. Result and Discussion

The theoretical model described here has been applied to Lead telluride nanowire. Figures 1a illustrate the variation of the power factor versus reduced Fermi energy for 125nm Lead telluride nano wire at 650K. The mode (n,m) = (1,1) data1 indicates that all sub-bands below or equal to (1,1) have been considered (x). As reduced fermi energy increased, value of power factor increased very slow attains a maximum value and

further decreases slowly. The mode (n,m) = (3,3) data2 indicates that all sub-bands below or equal to (3,3) have been considered (*). The mode (n,m) = (5,5) data3 indicates that all sub-bands below or equal to (5,5) have been considered (+). The mode (n,m) = (9,9) data4 indicates that all sub-bands below or equal to (9,9) have been considered (o). As number of sub-band increases, the power factor of PbTe nanowire increased and shifted towards high value of the Fermi energy. The maximum power factor of PbTe nanowire $0.022 W m^{-1} K^{-2}$ at $\xi = 0.5$. Figures 1b illustrate the variation of the power factor versus temperature at optimum reduced Fermi energy $\xi = 0.5$ for 125nm. For size quantum limits mode (n,m) = (1,1) data1 shows a constant behaviour with temperature. However as sub-bands contributes in transportation power factor increases linearly and become flats after 400K. If one consider the mode (n,m) = (9,9) data 4, power factor is optimum and long operating high temperature range found.

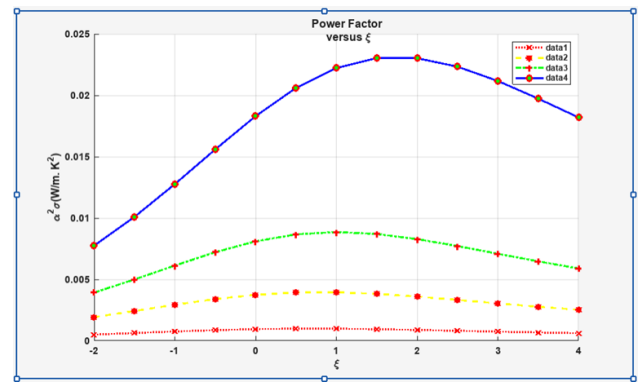


Fig. 1. Variation of power factor of PbTe nanowire with reduced fermi energy at 650K of 125nm cross sectional square size data1 refers mode (n,m) = (1,1) this indicates that all sub-bands below or equal to (1,1) have been considered (x); data2 refers mode (n,m) = (3,3) all sub-bands below or equal to (3,3) have been considered (*); data3 refers mode (n,m) = (5,5) indicates that all sub-bands below or equal to (5,5) have been considered (+); data4 refers mode (n,m) = (9,9) indicates that all sub-bands below or equal to (9,9) have been considered (o)

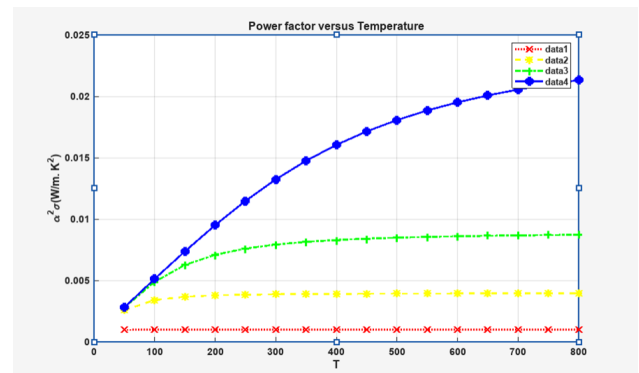


Fig. 2. Variation of power factor of PbTe nanowire with temperature at reduced fermi energy 0.5 of 120nm cross sectional square size data1 refers mode (n,m) = (1,1) this indicates that all sub-bands below or equal to (1,1) have been considered (x); data2 refers mode (n,m) = (3,3) all sub-bands below or equal to (3,3) have been considered (*); data3 refers mode (n,m) = (5,5) indicates that all sub-bands below or equal to (5,5) have been considered (+); data4 refers mode (n,m) = (9,9) indicates that all sub-bands below or equal to (9,9) have been considered (o)

Figure 2 Variation thermoelectric figure-of merits ZT of PbTe nanowire with cross sectional square size 'a' at temperature 650K and reduced Fermi energy 0.5 ; data1 refers mode (n,m) = (1,1) this indicates that all sub-bands below or equal to (1,1) have been considered (x); data2 refers mode (n,m) = (3,3) all sub-bands below or equal to (3,3) have been considered (*); data3 refers mode (n,m) = (5,5) indicates that all sub-bands below or equal to (5,5) have been considered (+); data4 refers mode (n,m) = (9,9) indicates that all sub-bands below or equal to (9,9) have been considered (o). As cross sectional size decreased, ZT increased attains a maxima and as number of sub-band increased maximum ZT shifted towards left side. The value of optimum ZT 2.7 at 650K at reduced Fermi energy $\xi = 0.5$.

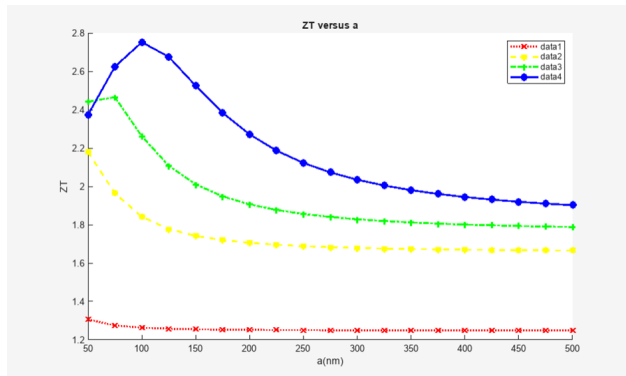


Fig. 3. Variation Thermoelectric figure-of merits ZT of PbTe nanowire with cross sectional square size 'a' at temperature 650K and reduced fermi energy 0.5 ; data1 refers mode (n,m) = (1,1) this indicates that all sub-bands below or equal to (1,1) have been considered (x); data2 refers mode (n,m) = (3,3) all sub-bands below or equal to (3,3) have been considered (*); data3 refers mode (n,m) = (5,5) indicates that all sub-bands below or equal to (5,5) have been considered (+); data4 refers mode (n,m) = (9,9) indicates that all sub-bands below or equal to (9,9) have been considered (o)

Figure 3 Variation Thermoelectric figure-of merits ZT of PbTe nanowire with temperature at reduced Fermi energy 0.5 of 120nm cross sectional square size. As temperature increases value of ZT increases become flats above 400K. The size quantum limits has lower value of ZT however as more sub-bands increased value of ZT increases and become optimum.

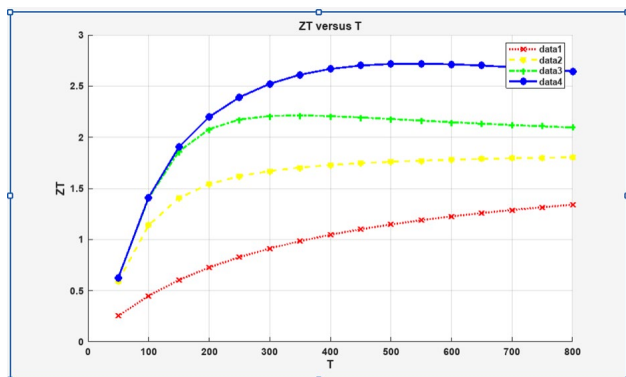


Fig. 4. Variation Thermoelectric figure-of merits ZT of PbTe nanowire with temperature at reduced fermi energy 0.5 of 120nm cross sectional square size

data1 refers mode (n,m) = (1,1) this indicates that all sub-bands below or equal to (1,1) have been considered (x); data2 refers mode (n,m) = (3,3) all sub-bands below or equal to (3,3) have been considered (*); data3 refers mode (n,m) = (5,5) indicates that all sub-bands below or equal to (5,5) have been considered (+); data4 refers mode (n,m) = (9,9) indicates that all sub-bands below or equal to (9,9) have been considered (o)

Figures 4 illustrate the variation of the dimensionless figure-of-merits ZT versus reduced fermi energy for 120nm PbTe nano wire at temperature 650K. As number of sub-band increases the maxima of ZT shifted towards the left side.

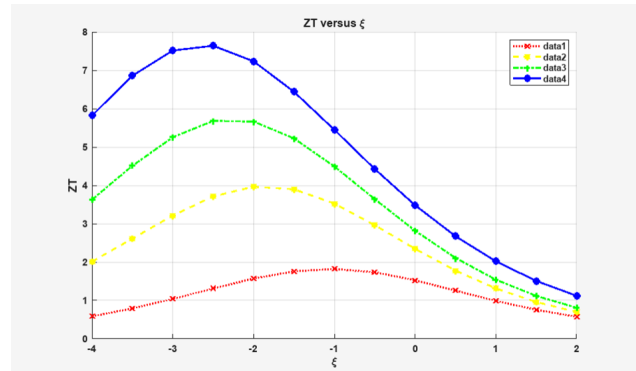


Fig. 5. Variation Thermoelectric figure-of merits ZT of PbTe nanowire with reduced fermi energy at temperature 650 K of 125nm cross sectional square size data1 refers mode (n,m) = (1,1) this indicates that all sub-bands below or equal to (1,1) have been considered (x); data2 refers mode (n,m) = (3,3) all sub-bands below or equal to (3,3) have been considered (*); data3 refers mode (n,m) = (5,5) indicates that all sub-bands below or equal to (5,5) have been considered (+); data4 refers mode (n,m) = (9,9) indicates that all sub-bands below or equal to (9,9) have been considered (o)

References

- [1] M. S. Dresselhaus et al, "Quantum wells and quantum wires for potentials thermoelectric Application" *Resent Trends in Thermoelectric Materials, Research III, Semiconductor and Semimetals*, (Academic Press,) Editor. Terry M. Tritt 71 (2001)
- [2] M.P. Singh and C.M. Bhandari , *Pramana: Journal of Physics* 62, No.6, (2004)1309
- [3] M.P. Singh and C.M. Bhandari, *Indian Pure and Applied Physics* 41, (2003)950
- [4] M.P. Singh and C.M. Bhandari, *Solid State Communications* 133,29 (2005)
- [5] M.P. Singh and C.M. Bhandari, *Solid State Comm* 127, 649 (2003).
- [6] Haoran Xue, Yang Yihao, and Zhang Baile. "Topological acoustics." *Nature Reviews Materials* 7.12 ,(2022)974
- [7] M.F.P. Wagner, A.S. Paulus, W. Sigle et al. *Sci Rep* 13, (2023)8290.
- [8] J. A. Hernandez, A. Ruiz, L.F. Fonseca et al. *Sci Rep* 8, 11966 (2018)11966. <https://doi.org/10.1038/s41598-018-30450-5>
- [9] Yong Lin, Huh daihong et al. *Nature communication* 12,(2021)3926
- [10] M.P. Singh, *International Journal of Science Engineering and Technology* Vol. 13 issue 2, 2025 DOI: [10.61463/ijset.vol.13.issue2.339](https://doi.org/10.61463/ijset.vol.13.issue2.339)
- [11] M.P. Singh, *International Journal of Science Engineering and Technology* Vol. 14 issue 1, 2026 DOI: <https://doi.org/10.5281/zenodo.18359379>
- [12] Mahendra Pratap Singh, *International Journal of Progressive Research in Science and Engineering*, 6(03), 24–26 (2025). <https://journal.ijprse.com/index.php/ijprse/article/view/1147>
- [13] M. P. Singh, *J. Phys. Commun.* 2 045021(2018) <https://doi.org/10.1088/2399-6528/aaec3>
- [14] X.Wang , J.Young et al. *Measurement of science and Technology* 29(2), (2018)025001
- [15] Jeongmin Kim Wooyoung Shim and Wooyoung Lee, *Journal of Materials Chemistry C*, 3, (2015)11999 doi:10.1039/c5tc02886h

- [16] Jose A. Hernandez et al *Scientific Report* 8,(2018)11966
- [17] Ou M. N. Yang T J et al. *Applied physics Letters* 92, (2008)063101.
Doi.10.1063/1.2839572
- [18] Hochbaum A I, et al. *Nature* 451, (2008)163.
- [19] A. Khitun, K.L. Wang and G.Chen *Nanotechnology* 11,(2000)327.
- [20] R.Venkatasubramanian, E. Siivola, T. Colpitts and B. O'Quinn B, *Nature* 413, (2001)597.
- [21] J.Lee and M.O. Vassell , *J. Phys C: Solid State Phys* 17,2525 (1984).